

## Growth And Characterisation Of Glycine Single Crystal

\*Gopala krishnamani , R, S, <sup>2</sup>Rajeswari, S and <sup>3</sup>Lalitha, S

\*Lecturer(SG) in physics, Seshasayee Institute of Technology, Trichy-10

<sup>1</sup>Assistant professor of physics, Periyar EVR college, Trichy-23

<sup>2</sup>Associate professor of physics, Periyar EVR college, Trichy-23

<sup>3</sup>Associate professor of physics, Periyar EVR college, Trichy-23

Corresponding Author: Gopala krishnamani

---

**Abstract:** The single crystal of Glycine is grown by slow evaporation method. Optimized geometrical structure and harmonic vibrational frequencies have been computed by the B3LYP density functional levels using 6-311++G(d,p) basis sets. The geometries and normal modes of vibration obtained from DFT method are compared with the literature values. The optical absorption and transmission spectrum are recorded in the range 190-1100nm. A detailed molecular picture of Glycine and its intermolecular interactions were obtained from NBO analysis. The paramagnetic behavior of the molecule under consideration has been investigated and the variation of paramagnetic susceptibility with temperature has been studied.

**Keywords:** Vibrational spectra, Geometrical parameters, Dipole-moment, NBO, Paramagnetic susceptibility, Glycine.

---

Date of Submission: 06-08-2018

Date of acceptance: 24-08-2018

---

### I. Introduction

Amino acids build proteins, and proteins are life-sustaining macronutrients. There are 10 amino acids identified as essential, although one of them, arginine, is really only essential for the young, according to Michael Davidson of the National High Magnetic Field Laboratory at Florida State University. The 10 essential amino acids are arginine, histidine, isoleucine, leucine, lysine, methionine, phenylalanine, threonine, tryptophan and valine.

Glycine is one of the non-essential amino acids and is used to help create muscle tissue and convert glucose into energy. It is also essential to maintaining healthy central nervous and digestive systems, and has recently been shown to provide protection via antioxidants from some types of cancer. Glycine is used in the body to help construct normal DNA and RNA strands—the genetic material needed for proper cellular function and formation. It helps prevent the breakdown of muscle by boosting the body's levels of creatinine, a compound that helps build muscle mass.

### GROWTH OF GLYCINE SINGLE CRYSTAL

Glycine were dissolved in double distilled water in the stoichiometric ratio 1:3 at room temperature. The solution was stirred well for 4 hours using a magnetic stirrer to obtain homogeneous mixture. Then the solution was filtered using Whatman filter paper, to remove the dust particles and undissolved materials. The filtered solution was allowed for evaporation to dryness at room temperature and the synthesized salt was obtained. The synthesized salt was used to prepare the saturated solution for crystal growth.

The saturated solution was maintained in the undistributed condition and the beaker was covered by polythene paper. Few holes were made on polythene cover for slow evaporation. By adopting the solution growth method single crystal of glycine was grown from super saturated solution at room temperature. Then this solution was periodically inspected and from 13 days onwards the crystal started growing. It was permitted to grow for another 13 days in order to get a nominal size suitable for characterization. The single crystal of glycine with dimension of 7mm×4mm×2mm was thus obtained. The grown single crystals of glycine are shown in figure 1.



Figure 1 Grown crystal of Glycine

### COMPUTATIONAL DETAILS

The entire vibrational assignments and the geometrical parameters are predicted by DET-B3LYP method with the standard basis set 6-311++G(d,p) level in Gaussian03W software package. By using the GAUSSVIEW Program the vibrational assignments were made.

## II. Results And Discussion

### *Molecular structure*

The geometrical structure of the molecule, Glycine is shown in Figure 2. The geometrical parameters are presented in the Table 1. The bond length related to C-H, C-O, N-H, C-C are all well agreement with the literature value(1). The value of the dihedral angle implies that all the atoms in the molecule are not in plane.

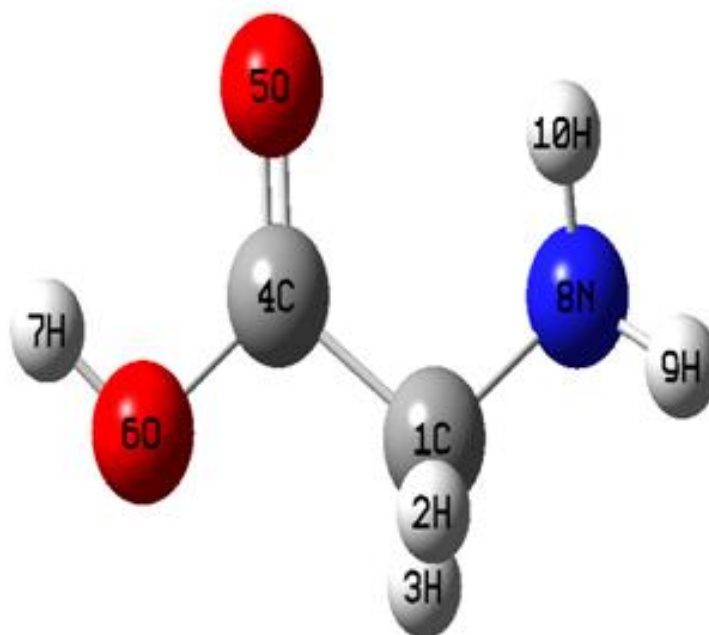


Figure 2 Geometrical structure of Glycine

**Table1** Geometrical parameters of Glycine

Parameter	Bond length	Parameter	Bond angle	Parameter	Dihedral angle
C <sub>1</sub> -H <sub>2</sub>	1.1033	H <sub>2</sub> -C <sub>1</sub> -H <sub>3</sub>	106.4592	H <sub>2</sub> -C <sub>1</sub> -C <sub>4</sub> -O <sub>5</sub>	104.9067
C <sub>1</sub> -H <sub>3</sub>	1.0935	H <sub>2</sub> -C <sub>1</sub> -C <sub>4</sub>	105.3271	H <sub>2</sub> -C <sub>1</sub> -C <sub>4</sub> -O <sub>6</sub>	-73.0166
C <sub>1</sub> -C <sub>4</sub>	1.5116	H <sub>2</sub> -C <sub>1</sub> -N <sub>8</sub>	114.9573	H <sub>3</sub> -C <sub>1</sub> -C <sub>4</sub> -O <sub>5</sub>	-141.4162
C <sub>1</sub> -N <sub>8</sub>	1.4546	H <sub>3</sub> -C <sub>1</sub> -C <sub>4</sub>	108.5122	H <sub>3</sub> -C <sub>1</sub> -C <sub>4</sub> -O <sub>6</sub>	40.6605
C <sub>4</sub> -O <sub>5</sub>	1.2048	H <sub>3</sub> -C <sub>1</sub> -N <sub>8</sub>	110.7612	N <sub>8</sub> -C <sub>1</sub> -C <sub>4</sub> -O <sub>5</sub>	-19.8047
C <sub>4</sub> -O <sub>6</sub>	1.3531	C <sub>4</sub> -C <sub>1</sub> -N <sub>8</sub>	110.7612	N <sub>8</sub> -C <sub>1</sub> -C <sub>4</sub> -O <sub>6</sub>	162.272
O <sub>7</sub> -H <sub>6</sub>	0.9692	C <sub>1</sub> -C <sub>4</sub> -O <sub>5</sub>	110.4868	H <sub>2</sub> -C <sub>1</sub> -N <sub>8</sub> -H <sub>9</sub>	40.3456
N <sub>8</sub> -H <sub>9</sub>	1.0124	C <sub>1</sub> -C <sub>4</sub> -O <sub>6</sub>	111.6695	H <sub>2</sub> -C <sub>1</sub> -N <sub>8</sub> -H <sub>10</sub>	-80.9218
N <sub>8</sub> -H <sub>10</sub>	1.0148	O <sub>5</sub> -C <sub>4</sub> -O <sub>6</sub>	123.0553	H <sub>3</sub> -C <sub>1</sub> -N <sub>8</sub> -H <sub>9</sub>	-80.3611
		C <sub>4</sub> -O <sub>6</sub> -H <sub>7</sub>	107.3244	H <sub>3</sub> -C <sub>1</sub> -N <sub>8</sub> -H <sub>10</sub>	158.3715
		C <sub>1</sub> -N <sub>8</sub> -H <sub>9</sub>	111.4860	C <sub>4</sub> -C <sub>1</sub> -N <sub>8</sub> -H <sub>9</sub>	159.3661
		C <sub>1</sub> -N <sub>8</sub> -H <sub>10</sub>	110.5141	C <sub>4</sub> -C <sub>1</sub> -N <sub>8</sub> -H <sub>10</sub>	38.0987
		H <sub>8</sub> -N <sub>8</sub> -H <sub>10</sub>	108.9039	C <sub>1</sub> -C <sub>4</sub> -O <sub>6</sub> -H <sub>7</sub>	176.9628
				O <sub>5</sub> -C <sub>4</sub> -O <sub>6</sub> -H <sub>7</sub>	-1.0136

### VIBRAATIONAL ASSIGNMENTS

Glycine molecule has 10 atoms with 24 fundamental vibrations. The fundamental vibrations are distributed as 17 in-plane vibration and 7 out-of-plane vibration. Table 3 summarize the fundamental modes of vibration, force constant, infrared intensity, Raman activity and polarization ratios of the molecule Glycine.

#### C-O Stretching and O-H Bending Vibration

The C-O stretching and O-H bending modes are not independent vibrational modes because they couple with the vibrations of adjacent groups. The C-O stretching mode is coupled with the adjacent C-C stretching vibration; thus in salicylic acid, the vibration might better be described as an asymmetric CCO stretching vibration. Two bands arising from C-O stretching and O-H bending appear in the spectra of carboxylic acids near 1210-1320 and 1400-1440 cm<sup>-1</sup>, respectively(2). In our study the band at 1145cm<sup>-1</sup> is due to C-O stretching and 1323 cm<sup>-1</sup> is due to O-H bending vibration. The theoretically calculated O-H stretching and out-of-plane bending vibrations are observed at 3759cm<sup>-1</sup> and 623cm<sup>-1</sup> respectively.

#### C=O Vibration

The appearance of a strong band in the spectrum between 1650-1950 cm<sup>-1</sup> shows the presence of a carbonyl group in the compound. It is due to C=O and is the most representative type of vibration localized in an individual bond(3). The frequency of absorption due to the carbonyl group depends mainly on the force constant which in turn depends upon inductive effect, conjugative effect, field effect and steric effects. In our study the C=O stretching vibration is observed at 1819 cm<sup>-1</sup>. The other vibration related to carbonyl group is presented in the Table2

#### CH<sub>2</sub> Vibration

For the assignments of CH<sub>2</sub> group frequencies, basically six fundamentals can be associated with each CH<sub>2</sub> group namely, CH<sub>2</sub> symmetric stretch; CH<sub>2</sub> asymmetric stretch, CH<sub>2</sub> scissoring and CH<sub>2</sub> rocking, which belong to in-plane vibrations and two out-of-plane vibrations, viz., CH<sub>2</sub> wagging and CH<sub>2</sub> twisting modes, which are expected to be depolarized(4). The asymmetric CH<sub>2</sub> stretching vibrations are generally observed above 3000 cm<sup>-1</sup>, while the symmetric stretch will appear between 3000 and 2900 cm<sup>-1</sup>. The C-H stretching vibration modes are obtained theoretically at 3063 cm<sup>-1</sup> and 2946 cm<sup>-1</sup>. The band obtained at 1492 cm<sup>-1</sup> is due to CH<sub>2</sub> scissoring one. The CH<sub>2</sub> wagging vibration is obtained at 1445 cm<sup>-1</sup>. The band at 1020cm<sup>-1</sup> is due to CH<sub>2</sub> rocking vibration. The torsional vibration of CH<sub>2</sub> is obtained 97cm<sup>-1</sup>.

#### NH<sub>2</sub> Vibrations

The N-H stretches of amines are in the region 3300-3000 cm<sup>-1</sup>. These bands are weaker and sharper than those of the alcohol O-H stretches which appear in the same region. In primary amines (RNH<sub>2</sub>), there are two bands in this region, the asymmetrical N-H stretch and the symmetrical N-H stretch. The N-H bending vibration of primary amines is observed in the region 1650-1580 cm<sup>-1</sup>(5). Another band attributed to amines is observed in the region 910-665 cm<sup>-1</sup>. This strong, broad band is due to N-H wagging and observed only for primary and secondary amines(6).

C-N stretching vibration of aliphatic amines is observed as medium or weak bands in the region 1250-1020 cm<sup>-1</sup>. In aromatic amines, the band is usually strong and in the region 1335-1250 cm<sup>-1</sup>. The asymmetrical and

symmetrical NH<sub>2</sub> vibration is obtained at 3605 cm<sup>-1</sup> and 3517cm<sup>-1</sup> respectively. The scissoring and wagging vibration of NH<sub>2</sub> group is observed theoretically at 1643 cm<sup>-1</sup> and 815cm<sup>-1</sup> respectively. The rocking NH<sub>2</sub> vibration is obtained at 1219cm<sup>-1</sup>. The band at 1105cm<sup>-1</sup> is due to C-N stretching vibration. The correlation graph of IR intensity and Raman activity with wave numbers are presented in Figure 3 and 4 respectively.

**Table 2**vibrational assignments of glycine.

Frequency	Reducedmass	Force constant	IR intensity	Raman activity	Depolarization ratio		Vibrational assignments
					(P)	(U)	
3605	1.0939	8.3553	12.3939	48.3179	0.6248	0.769	NH <sub>2</sub> asym
3517	1.0497	7.6493	4.6614	107.3025	0.0833	0.1537	NH <sub>2</sub> sym
3063	1.0854	6.0018	14.2389	89.2756	0.3125	0.4762	C-H STR
2946	1.0739	5.4906	46.5218	135.4696	0.2116	0.3492	C-H STR
1819	8.6769	16.9123	307.6727	10.966	0.1461	0.2549	C=O
1643	1.1104	1.7561	67.3781	2.8475	0.5978	0.7483	NH <sub>2</sub> SCISS
1492	1.0804	1.417	11.4364	11.509	0.6885	0.8155	CH <sub>2</sub> SCISS
1445	1.7948	2.2083	23.0252	1.6169	0.1182	0.2140	CH <sub>2</sub> WAGG
1323	1.7126	1.7654	29.1625	3.2551	0.7484	0.8561	O-H BEND
1261	1.2432	1.1642	0.2142	5.2252	0.7494	0.8567	C-H BEND
1219	1.4667	1.2836	59.7443	5.8606	0.577	0.7318	NH <sub>2</sub> ROCK
1144	1.7567	1.3544	218.027	1.7115	0.7485	0.8561	C-O STR
1105	2.7671	2.0129	62.0955	3.5081	0.4864	0.6077	C-NSTR
1020	2.2156	1.3577	3.4406	1.301	0.6894	0.8162	CH <sub>2</sub> ROCK
840	3.1733	1.3197	13.5662	8.8461	0.0895	0.1642	C-CSTR
815	1.2473	0.4877	185.1018	1.3959	0.4258	0.5973	NH <sub>2</sub> WAGGING
662	2.0241	0.5227	74.651	1.869	0.2549	0.4062	C-C-OBEND
623	2.5058	0.5733	41.5852	1.5574	0.653	0.7896	C=O BEND
517	1.6911	0.2648	32.4286	1.9242	0.7483	0.856	OH BEND
464	4.2286	0.5369	14.1387	1.8846	0.4871	0.6551	CCN BEND
282	4.5548	0.2131	1.3714	0.3414	0.7456	0.8543	NCN BEND
180	1.0771	0.0206	50.3544	0.261	0.4523	0.6229	NH <sub>2</sub> TWIST
97.1	2.6622	0.0148	1.1162	0.3292	0.5436	0.7044	CH <sub>2</sub> TWIST

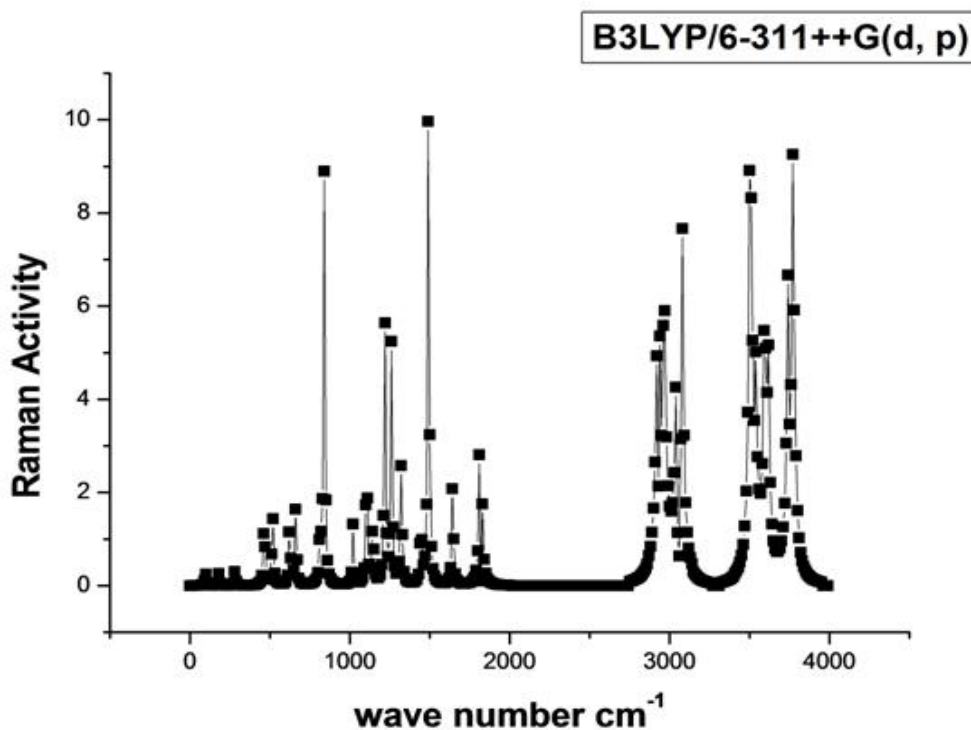


**Figure 3**Correlation graph of Raman activity with wave number

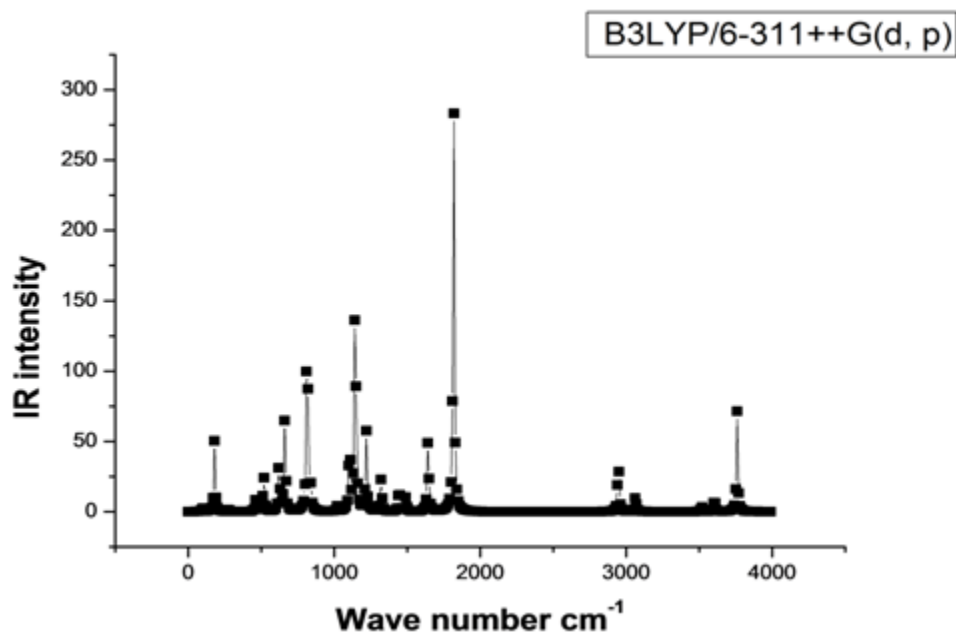


Figure 4 Correlation graph of IR intensity with wave number

**UV-VIS –NIR SPECTRAL STUDIES OF GLYCINE**

The transmission spectra are very important for any NLO materials because a NLO material can be of particular use only if it has a wide transparency window. The optical absorption and transmission spectrum are recorded in the range 190-1100nm using variation carry 5E spectrophotometer. The UV-Visible –NIR transmission and absorption spectrum are show in figure4 and figure5 respectively. The grown glycine crystal exhibits high transparency within the range of 240-1100nm. The lower cut off frequency is around 204nm and greater transparency makes it a suitable material for optoelectronic applications.

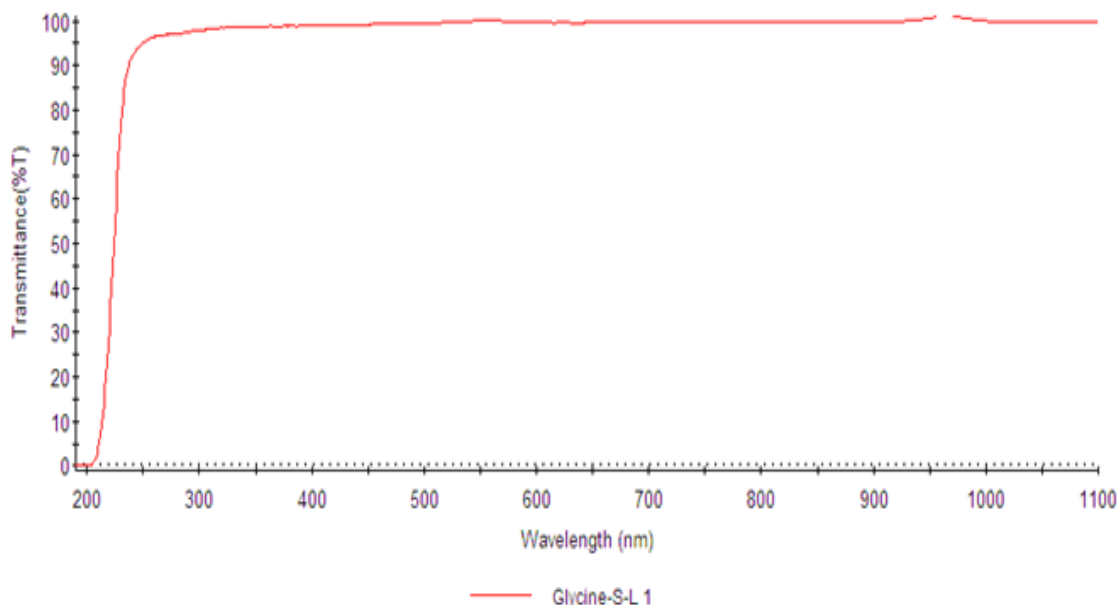
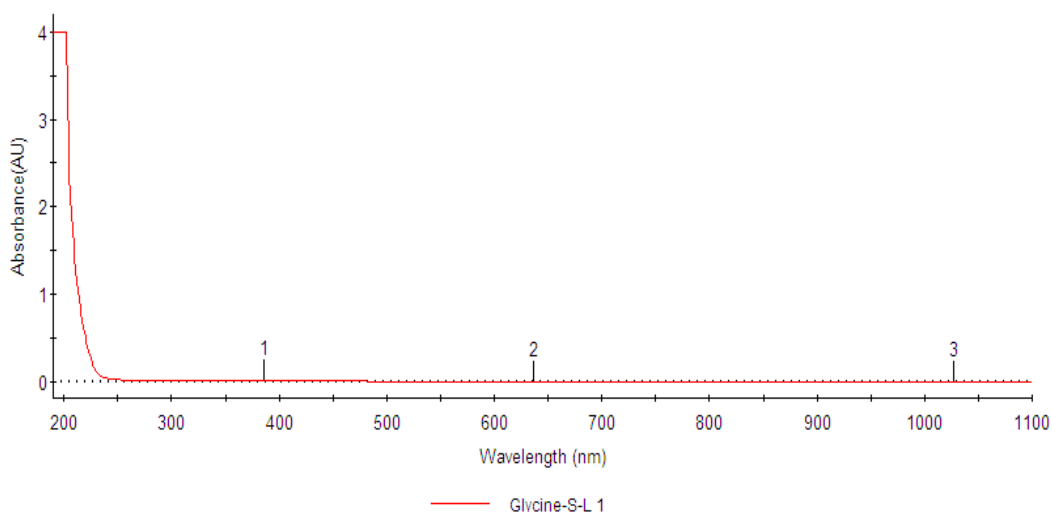


Figure 5UV-VIS-NIR Transmittance spectrum of glycine



**Figure 6** UV-VIS-NIR Absorbance spectrum of glycine

### Dipole moment

The dipole moment was also calculated with B3LYP/6-311++G(d,p) basis set. Dipole moment reflects the molecular charge distribution and is given as a vector in three dimensions. Therefore it can be used as descriptor to depict the charge movement across the molecules depends on the centres of positive and negative charges. Dipole moments are strictly determined for neutral molecules. For charged systems, its values depend on the choice of origin and molecular orientation.

Electron density of the ring is decreased by the electron withdrawing inductive effect of the electronegative nitrogen atom. Thus the molecule has a substantial dipole moment (2.8638 Debye) with the ring carbons acting as positive end of the dipole. The dipole moment of a bond depends on differences in electronegativity between the two atoms in the bond. The dipole moment of a molecule is then the resultant vector of all the bond dipoles. Lone pairs contribute to the molecule's dipole moment even though they do not constitute a bond. Clearly the nucleus end of the lone pair is positive and the electron end is negative so one might think of a 'lone pair dipole' contributing to the polarity of the molecule in analogy to bond dipole. The lone-pair electrons on the nitrogen atom stick out into space away from the positively charged nucleus which gives rise to a dipole moment.

### Nbo analysis

Bond formations between the atoms due to the overlap of different hybrids and NBO occupancies at bond critical points are listed in Table 3. The lone pair of electrons of the oxygen atom extends in the plane of the molecule. The  $sp^2$  hybridization is to allow one of the lone pairs of oxygen to reside in a p orbital and thus allow it to interact within the p-system. The NBO occupancies of C4-O6 bond is larger than those of other bonds indicating that the strength of C4-O6 bond is larger than those of other bonds. The larger differences in electronegativity of the atoms involved in the bond formation are reflected in the larger differences in the polarization coefficients of the atoms. The difference in polarization coefficients is small when similar atoms are involved in bond formation (CC bond) whereas appreciable differences are found in CO bond formation. Electronegativity values are largely reflected in the polarization coefficients of the corresponding bond. A serial number (1, 2) represents whether there is a single or a double bond. BD (1) represents that a single bond is formed between the atoms and the composition of the hybrids shows that all single bonds are  $\sigma$  bonds, which are due to the overlap of  $sp^2$  hybrids, and for BD (2), the composition shows that one bond in all the double bonds is a  $\pi$  bond, which is due to the lateral overlap of two p orbitals. NBO analysis shows that the occupancy is much reduced in the corresponding antibonding orbital of the  $\sigma$  bond, and it is increased in the anti-bonding orbital of the  $\pi$  bond.

**Table 3** Hybrid compositions of Glycine.

BOND (A-B)	ED/ENERGY	NBO
BD(1) C1-C4	1.97188	0.7062( $sp^{1.74}$ )+0.7080( $sp^{1.76}$ )
BD*(1) C1-C4	0.01259	0.7080( $sp^{1.74}$ )-0.7062( $sp^{1.76}$ )

BD(1) C4-O6	1.98884	0.8291(sp <sup>2.22</sup> )+0.5591(sp <sup>1.99</sup> )
BD*(1) C4-O6	0.00359	0.5591(sp <sup>2.22</sup> )-0.8291(sp <sup>1.99</sup> )
BD(1) O6-H7	1.98816	0.8570(sp <sup>3.91</sup> )+0.5153(s)
BD*(1) O6-H7	0.00707	0.5153(sp <sup>3.91</sup> )-0.8570(s)
BD(2) C4-O5	1.81918	0.7330(p)+0.6803(p)
BD*(2) C1-C2	0.28582	0.6803(p)-0.7330(p)

**Magnetic properties**

Magnetic susceptibility results from the response of electronic orbits and/or unpaired spins to an applied field. In paramagnetic materials  $\chi$  is positive-that is, for which  $M$  is parallel to  $B$ . The susceptibility is however is also very small:  $10^{-4}$  to  $10^{-5}$ . The fact that these compounds have incomplete atomic shells is what is responsible for their paramagnetic behavior. They all have a critical temperature below which the variation of susceptibility with temperature is very different from its variation above this temperature. Paramagnetism derives from the spin and orbital

angular momenta of electrons. This type of magnetism occurs only in compounds containing unpaired electrons, as the spin and orbital angular momenta are cancelled out when the electrons exist in pairs. A plot of  $1/\chi$  vs. temperature is known as a Curie plot. Ideally, it should be linear if the Curie-Weiss law is obeyed. From such a plot, we can then extract the Curie constant from the inverse of the slope and the Weiss constant from the x-intercept(7,8) For Glycine, Table 4 shows the variation of susceptibility with temperature and Figure 7 shows the Curie plot. The plot shows that Glycine is paramagnetic in nature.

Curie constant = 0.000126,

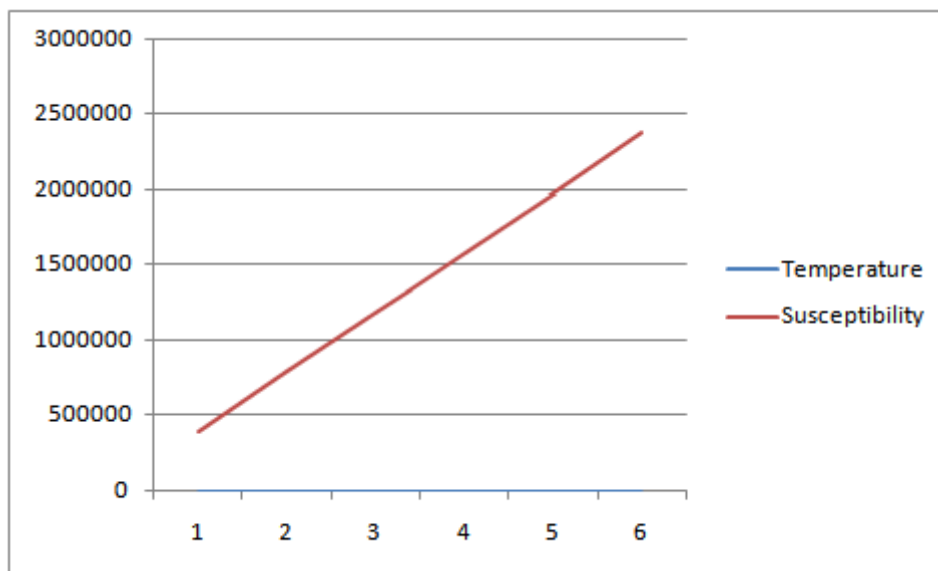
Weiss constant =  $1.26^{-13}$ .

The Weiss constant is almost zero. Hence the plot passes through the origin which proves the paramagnetic nature of Glycine.

**Table 4** Curie plot of Glycine

Temperature	Susceptibility
50	397456.2
100	794912.5
150	1192368.8
200	1589825.1
250	1987281.4
300	2384737.7

**Figure 7** Curie plot of Glycine



### **III. Conclusion**

The present investigation thoroughly analyzed the vibrational spectra, both infrared and Raman of glycine. All the vibrational bands observed in the FT-IR and FT-Raman spectra of the title compound are assigned to the various modes of vibration. Most of the modes have

wavenumbers in the range suggested by previous assignments found in literature in the case of related molecules. The UV cut off wavelength was found to be 204nm. The crystal exhibits low absorption in the entire visible and NIR region and as it is one of the desired properties for the crystals utilized for NLO device fabrication. The NBO analysis confirms the hyperconjugation interaction. The strengthening and increase in wavenumber is due to the hyperconjugation interaction. The presence of lone pair of electrons in Glycine is responsible for paramagnetic nature of the molecule.

### **References**

- [1]. H.S.Randhawa, Modern Molecular Spectroscopy, Macmillan India Limited, 2003.S
- [2]. Y.R. Sharma, Elementary Organic Spectroscopy Principles and Applications, S.Chand &Company Ltd, 2007.
- [3]. Barbara Stuart, Infrared Spectroscopy: Fundamentals and Applications, Wiley publications, 2004.
- [4]. Mool chand Gupta, Atomic and Molecular Spectroscopy, New Age International Publishers, New Delhi, 2007.
- [5]. G.Socrates, Infrared Characteristic Group Frequencies, John Wiley, GB, 1980.
- [6]. S.Seshadri, S.Gunasekaran, S.Muthu, S.Kumaresan, R.Arun Balaji, J.Raman Spectrosc.38 (2007)1523-1531.
- [7]. V. Balachandran, S.Rajeswari, S. Lalitha, Spectrochim. Acta, 113A (2013) 268-280
- [8]. J.H. Van Vleck, The Theory of Electric and Magnetic Susceptibilities, Oxford University Press, Oxford, 1932.

IOSR Journal of Applied Physics (IOSR-JAP) is UGC approved Journal with Sl. No. 5010, Journal no. 49054.

Gopala krishnamani "Growth And Characterisation Of Glycine Single Crystal." IOSR Journal of Applied Physics (IOSR-JAP) , vol. 10, no. 4, 2018, pp. 72-79